Biochimica et Biophysica Acta, 1107 (1992) 44–54

BBAMEM 75631

Effects of lung surfactant proteolipid SP-C on the organization of model membrane lipids: a fluorescence study

Ann D. Horowitz, Barry Elledge, Jeffrey A. Whitsett and John E. Baatz

Division of Pulmonary Biology, Children's Hospital Medical Center, Elland and Bethesda Avenues, Cincinnati, OH (USA)

(Received 12 November 1991)
(Revised manuscript received 26 February 1992)

Key words: Surfactant; Fluorescence; Lipid–protein interaction; Model membrane

Lipid–protein interactions of pulmonary surfactant-associated protein SP-C in model DPPC/DPPG and DPPC/DPPG/eggPC vesicles were studied using steady-state and time-resolved fluorescence measurements of two fluorescent phospholipid probes, NBD-PC and NBD-PG. These fluorescent probes were utilized to determine SP-C-induced lipid perturbations near the bilayer surface, and to investigate possible lipid headgroup-specific interactions of SP-C. The presence of SP-C in DPPC/DPPG membrane vesicles resulted in (1) a dramatic increase in steady-state anisotropy of NBD-PC and NBD-PG at gel phase temperatures, (2) a broadening of the gel-fluid phase transition, (3) a decrease in self-quenching of NBD-PC and NBD-PG probes, and (4) a slight increase in steady-state anisotropy of NBD-PG at fluid phase temperatures. Time-resolved measurements, as well as steady-state intensity measurements indicate that incorporation of SP-C into DPPC/DPPG or DPPC/DPPG/eggPC vesicles results in a increase in the fraction of the long-lifetime species of NBD-PC. The results presented here indicate that SP-C orders the membrane bilayer surface, disrupts acyl chain packing, and may increase the lateral pressure within the bilayer.

Introduction

Pulmonary surfactant is a lipid-protein complex secreted by Type II epithelial cells lining the alveoli of the lung. The phospholipid components, primarily phosphatidylcholine and phosphatidylglycerol, are believed to form a monolayer film at the air/liquid interface which dramatically lowers surface tension within the alveolus, thereby preventing collapse of the distal components of the lung [1,2]. Surfactant deficiency, manifest clinically as respiratory distress syndrome (RDS), is a frequent cause of morbidity and mortality in premature infants.

Although phospholipids are inherently surface-active, physiologically useful surfactants must be effective in the dynamic environment of the lung. Since alveoli expand and contract during the respiratory cycle, an efficient surfactant must adsorb rapidly to the surface, and respread quickly after compression [3,4]. In addition, the surfactant monolayer must withstand high compressive forces in order to generate the requisite low surface tension. Pulmonary surfactant is enriched in saturated phospholipids, such as dipalmitoylphosphatidylcholine (DPPC), that are well able to withstand lateral compression at temperatures below their gel to fluid phase transition (T_m); however, such lipids adsorb and respread poorly [1,5,6]. By contrast, unsaturated phospholipids exhibit much better dynamic properties but cannot achieve low surface tension values. Although numerous investigators have attempted to create synthetic surfactant using lipid mixtures, including mixtures modelled upon the composition of natural surfactant, synthetic surfactant with properties identical to the natural product have not been achieved. In contrast to synthetic lipid surfactant, organic extracts of pulmonary surfactant have surface activity comparable to that of natural surfactant.

Two small hydrophobic surfactant-associated proteins, SP-B (M_r = 8700, monomeric form) and SP-C

Abbreviations: DPPC, 1,2-di-palmitoyl-*sn*-glycero-3-phosphocholine; DPPG, 1,2-dipalmitoyl-*sn*-glycero-3-phospho-*sn*-glycerol; NBD, 7-nitrobenz-2-oxa-1,3-diazol-4-yl; NBD-PC, 1-palmitoyl-2-(6-[*N*-(7 nitrobenz-2-oxa-1,3-diazol-4-yl)amino]caproyl)-*sn*-glycero-3-phosphocholine; NBD-PG, 1-palmitoyl-2-(6-[*N*-(7-nitrobenz-2-oxa-1,3-diazol-4-yl)amino]caproyl)-*sn*-glycero-3-phospho-*sn*-glycerol; eggPC, phosphatidylcholine from egg yolk, Mops, 4-morpholinepropanesulfonic acid.

Correspondence: J.E. Baatz, Children's Hospital Medical Center, Children's Hospital Research Foundation, Division of Pulmonary Biology, Elland and Bethesda Avenue, Cincinnati, OH 45229-2899, USA.

(M_r = 4200), exist as minor components in pulmonary surfactant and organic solvent extracts of whole surfactant [7–9]. These proteins contain predominantly hydrophobic domains and are derived from larger precursor proteins from which the more hydrophilic regions have been cleaved. The smaller proteolipid, SP-C, is 34 amino acid residues in length in its mature form, and is very rich in valine, leucine and isoleucine [7,10,11]. In addition, palmitoyl groups are covalently attached to the adjacent cysteines of SP-C [12]. The larger protein, SP-B, contains 79 residues and is somewhat more polar than SP-C [13,14]. When recombined into vesicles with synthetic phospholipids, SP-C confers surfactant activity comparable to that of natural surfactant both in vitro and in vivo [15]. Since preparations of SP-C and phospholipids are active at SP-C concentrations of 0.2% (w/w, protein/lipid) or less [15], and the surfactant material comprises mainly lipid rather than protein, the pronounced enhancement of activity observed in the presence of SP-C must reflect lipid reorganization induced by the protein.

In order to determine the effect of SP-C on phospholipid structure, steady-state and time-resolved fluorescence polarization measurements were performed on model phospholipid vesicles labeled with fluorescent probes and containing purified bovine SP-C at physiologically relevant concentrations. Such measurements permit the determination of the rate of rotational depolarization of the fluorophore embedded within the phospholipid bilayer. Effects of SP-C on the structure of lipid bilayers are likely to be reflected by changes in the motional freedom of a lipophilic probe. Fluorescence lifetimes and time-resolved fluorescence anisotropies were therefore determined for fluorescent phospholipid probes in model phospholipid vesicles at temperatures below and above T_m in order to distinguish gel phase and fluid phase effects of the SP-C protein.

The fluorescent probe NBD-PC has been used to label phospholipid vesicles and trace their intracellular routing in reuptake experiments by fluorescence microscopy [16,17]. In addition to the intense emission and large Stokes shift which make NBD-PC valuable for microscopy, the NBD fluorophore is a useful reporter of its local environment, since the quantum yield and wavelength of emission are strongly dependent on polarity. NBD-containing probes are highly sensitive to self-quenching effects in high concentrations or when concentrated in domains [25]. NBD-PC has been widely used as a reporter of lipid bilayer structure and for lipid–protein interactions [18]. Unlike more hydrophobic membrane probes, it is sensitive to perturbations at the surface, rather than the interior, of the bilayer. In the experiments reported here, NBD-PC was used to label vesicles for time-resolved and steady-state anisotropy measurements in order to obtain information on lipid–protein interactions of bovine SP-C.

Experimental methods

Purification of SP-C

SP-C was isolated from cow lungs by methods described previously [7]. Briefly, freshly excised lungs were lavaged with 0.15 M saline and surfactant was pelleted by centrifugation. Surfactant was extracted with 2:1 (v/v) diethyl ether/ethanol or $CHCl_3$/CH_3OH, and the extract was dialyzed against the same solvent. SP-C was purified from the dialysate by passing the dialysate through a silica column using a stepwise gradient of chloroform/methanol. Prolonged dialysis in chloroform/methanol/0.01 M HCl was utilized to remove contaminating lipids and protein. Silica column chromatography and dialysis were repeated until a sufficiently pure preparation of SP-C was obtained. In the final dialysis step, the purified SP-C was dialyzed against 2:1 (v/v) chloroform methanol to remove the HCl. SP-C was stored as a $CHCl_3/CH_3OH$ (2:1, v/v) solution. Purity of SP-C was determined by SDS-PAGE analysis and SP-C concentration was estimated by amino acid compositional analysis as described elsewhere [19]. SP-C generated by this methodology contained no detectable SP-B as assessed by ELISA or Western blot analysis using SP-B specific antisera.

Preparation of multilamellar vesicles

Stock solutions of phospholipids (Sigma Chemical Co., St. Louis) in chloroform were mixed to give a final molar ratio of 6:1:1 DPPC/DPPG/eggPC or 7:1 DPPC/DPPG. SP-C in 2:1 (v/v) chloroform/methanol solution was added to give the concentration desired (0 to 4% w/w SP-C with respect to total lipid). The lipids or protein/lipid mixtures were warmed at 45°C while being dried under a gentle stream of nitrogen. 2 ml of buffer, at 45°C, consisting of 10 mM Mops, 120 mM NaCl, 2 mM EDTA (pH 7.0) was added to the dried film. The samples were incubated for 30 min at 50°C. A volume of 0.3–0.5 μl of a 1 mg ml^{-1} NBD-probe/$CHCl_3$ stock solution was added either after addition of the 10 mM Mops buffer (as applies to most preparations used), or before solvent evaporation of lipid/protein organic solutions as specified in the text. Concentrations of NBD-PC and NBD-PG stock solutions were determined by measuring the absorbance at 460 nm in methanol, using $\epsilon_{480} = 2 \cdot 10^4$ cm^{-1} M^{-1} [18]. The final dye/lipid mole ratio was approximately 0.15% (or 1:700). The fluorescent probe was dispersed by brief sonication and vortexing, and the samples were incubated an additional 5 min at 50°C. Multilamellar vesicles were formed upon vortexing for 30 s as described previously [20–22]. The vesicles were then soni-

cated for 30 s in an EM/C bath ultrasonicator at room temperature in order to reduce aggregation of vesicles. For experiments requiring unilamellar vesicles, multilamellar dispersions were sonicated at 60 watts for 2 min at 0°C using a Braun Sonic 2000 sonicator equipped with a 5 mm microtip.

In order to estimate the maximum possible fluorescence contributed by free NBD-probe (i.e., probe not associated with vesicles), 1 μl of 0.22 mM NBD-PC in ethanol was injected into 2 ml of the Mops buffer within a stirred cuvette at 30°C.

Steady-state fluorescence

For steady-state measurements, samples were transferred to quartz cuvettes and placed in the sample chamber of a Perkin-Elmer LS-50 fluorometer, which was maintained at the initial temperature of the experiment with a Lauda circulating water bath. The samples were allowed to equilibrate at this temperature for at least 30 min, with gentle stirring. For NBD-PC, excitation was at 465 nm and emission at 529 nm. For NBD-PG, excitation was at 463 nm and emission at 530 nm. In order to allow comparison of fluorescence intensities among samples in a single experiment, Triton X-100 was added at the end of the experiment from a 10% (w/v) stock solution to give a final concentration of 1%, at 50°C.

In the determinations of the error in anisotropy values resulting from free NBD-probe, the uncorrected anisotropy r_u and the corrected anisotropy r_c were calculated as follows:

$$r_u = \frac{I^t_{vv} - (G \cdot I^t_{vh})}{I^t_{vv} + (2G \cdot I^t_{vh})}$$

$$r_c = \frac{(I^w_{vv} - I^f_{vv}) - G \cdot (I^w_{vh} - I^f_{vh})}{(I^t_{vv} - I^f_{vv}) + 2G \cdot (I^w_{vh} - I^f_{vh})}$$

where I_{vv} and I_{vh} are the parallel and perpendicular components of fluorescence observed respectively, with the superscripts 'f' and 'l' denoting whether the samples were free NBD-PC, or liposomes containing NBD-PC, respectively, and G is the anistropy correction factor. The maximum percent error that could be introduced by the free dye is calculated to be:

$$\%e_{max} = \frac{r_u - r_c}{r_u} \times 100$$

The correction to the anistropy obtained by this method will be greater than the actual contribution of free NBD probe to the observed anistropy. This method was used to estimate the maximum possible error introduced by unbound probe.

Self-quenching experiments

For self-quenching experiments, multilamellar vesicles were formed as described above, except that the NBD-PC or NBD-PG probes were mixed with lipids and protein in chloroform/methanol prior to drying under N_2. Final lipid concentrations were 0.2 mM. Steady-state fluorescence intensity and anisotropy of the vesicles were recorded at 20°C. An aliquot of 10% Triton X-100 (Calbiochem) at 50°C was added to bring the final concentration to 1%. Samples were incubated with stirring for at least one-half hour to ensure dissolution of vesicles. Fluorescence in the presence of Triton was also recorded at 20°C. The ratio of fluorescence intensity in vesicles to fluorescence in 1% Triton X-100 was corrected for dilution to give F_v/F_T. The ratio of the fluorescence intensity of NBD probe in vesicles in the absence of self-quenching to the fluorescence in Triton X-100, $(F_v/F_T)_0$, was obtained by extrapolating the curve of (F_v/F_T) vs. mol% NBD probe back to zero mol%. The percent of fluorescence quenching at each probe concentration (%Q) was then calculated according to:

$$\%Q = \left(1 - \frac{(F_v/F_T)}{(F_v/F_T)_0}\right) \times 100\%$$

In some experiments, NBD probe concentrations were sufficiently high that the reduction in fluorescence due to the inner filter effect became significant (those in which the mol% NBD probe exceeded 1%). In those experiments, the optical density of the samples in 1% Triton X-100 at the excitation and emission wavelengths (OD_{ex} and OD_{em}) were measured following the completion of fluorescence measurements. Corrected fluorescence intensities were obtained according to:

$$F_{corr} = F_{obs} \cdot \text{antilog}\left(\frac{OD_{ex} + OD_{em}}{2}\right)$$

where F_{obs} is the observed and F_{corr} is the corrected fluorescence intensity. F_{corr} was then used for all fluorescence calculations.

Time-resolved fluorescence

Frequency-domain fluorescence measurements were performed at the Center for Fluorescence Dynamics, University of Illinois at Champaign-Urbana, on a modified instrument employing SLM480 T-format optics mated to a variable-frequency modulator and controlled by desktop computer using custom software. A nitrogen laser provided excitation at 325 nm. Excitation light was modulated at several frequencies between 1 and 160 MHz to permit resolution of multi-exponential lifetime decays by the phase-shift technique

[23]. In order to measure rotational correlation times, the phase angle differences and modulated amplitude ratios between horizontally and vertically polarized components of the emission at 490 nm were determined in paired measurements with emission polarizers alternately parallel and perpendicular. The polarized phase and modulation data were compared to values predicted for isotropic, anisotropic, and hindered rotator models given by the following expressions [24]:
for an isotropic rotator,

$$r(t) = r_0 e^{-t/\theta} \quad (1)$$

for an anisotropic rotator,

$$r(t) = r_0 \sum_i g_i e^{-t/\theta} \quad (2)$$

and for a hindered anisotropic rotator,

$$r(t) = (r - r_\infty) e^{-t/\theta} + r_\infty \quad (3)$$

where $r(t)$ is the emission anisotropy at time t after fluorescence excitation, r_0 is the limiting anisotropy which would be observed in the absence of depolarizing rotations, and θ_i is the correlation time for the ith depolarizing rotation. The g factors indicate the fraction of the limiting anisotropy dissipated by each depolarizing rotation, where $\Sigma g_i = 1$. Hindered rotations are modeled by including r_∞, which indicates residual anisotropy persisting at times much longer than the fluorescence lifetime. A nonlinear least-squares fit between the experimental results and the correlation times predicted for a particular model were calculated using the ISS187 computer program, ISS Instruments, Urbana, IL. χ^2 values were used to evaluate the relative appropriateness of a given model. In all cases, since NBD-PC was incorporated into phospholipid bilayers, the NBD probe was modelled best as a hindered anisotropic rotator (Eqn. 3). Maximum anisotropy (r_0), was measured in glycerol at 0°C.

Results

Steady-state fluorescence

The temperature-dependence of the steady-state anisotropy of NBD-PC in 7:1 DPPC/DPPG (mol/mol) multilamellar vesicles as a function of bovine SP-C concentration and temperature is shown in Fig. 1A. The anisotropy curve of NBD-PC in lipid only is characterized by a sharp decrease in anisotropy from 38°C to 42°C, with an inflection point at 41°C corresponding to the gel/fluid phase transition temperature (T_m) of 7:1 DPPC/DPPG membranes. Upon incorporation of increasing amounts of SP-C, substantial broadening of the phase transition occurred. At temperatures below the gel/fluid transition of DPPC/DPPG, specifically in the range of 20°C to 32°C, addition of SP-C resulted in marked increases in NBD-PC anisotropy. This increase is apparent at 0.5% (w/w) protein with respect to lipid, corresponding to a molar ratio of 1:1120 (protein/lipid). Above the gel-fluid phase transition temperature, an increase in anisotropy was often observed, but not reproducible. The effect of the presence of SP-C on the anisotropy of NBD-PG in 7:1 DPPC/DPPG vesicles at gel phase temperatures (Fig. 1B) was nearly identical to that observed for the NBD-PC probe over the same temperature range (20–38°C) in that anisotropy increased with increasing SP-C concentration. In the fluid phase (42–50°C), NBD-PG exhibited a small, but reproducible, increase in anisotropy at the highest concentration of SP-C examined (2% (w/w)). No hysteresis was observed upon cooling the samples from 50°C to 20°C (data not shown).

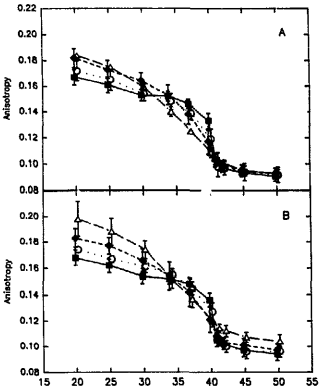

Fig. 1. Steady-state fluorescence anisotropy of (A) NBD-PC and (B) NBD-PG in 7:1 DPPC/DPPG multilamellar vesicles as a function of temperature and SP-C concentration. SP-C concentrations are: 0% (■), 0.5% (○), 1.0% (◆), and 2.0% (△) (w/w, protein/lipid). Total lipid concentrations were 0.15 mg/ml. For NBD-PC (A) excitation was at 465 nm and emission was recorded at 529 nm. For NBD-PG (B) excitation was at 463 nm and emission at 530 nm. The data points represent the average of three or four experiments, and the error bars represent the standard deviations of the data for each point. For clarity data points have been staggered slightly (0.2 C°).

The data presented in Fig. 1 were obtained from 3–4 preparations at each SP-C concentration. Each experiment examined four samples in parallel, containing 0, 0.5, 1.0 and 2.0% SP-C (w/w protein to lipid). The increase in anisotropy as a function of SP-C con-

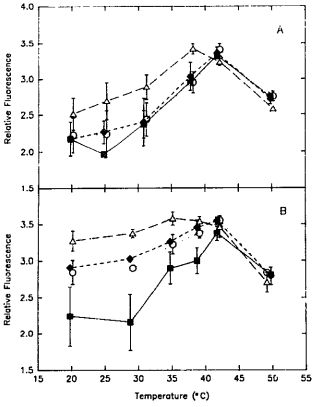

Fig. 2. Relative fluorescence intensity of (A) NBD-PC and (B) NBD-PG in 7:1 DPPC/DPPG multilamellar vesicles as a function of temperature and SP-C concentration. The fluorescence intensities are displayed as the ratio of the fluorescence at each temperature to the fluorescence of the sample at 50°C in the presence of 1% Triton X-100, (not corrected for dilution). SP-C concentrations are: 0% (■), 0.5% (○), 1.0% (◆), and 2.0% (△) (w/w, protein/lipid). Total lipid concentrations were 0.15 mg/ml. For NBD-PC (A) excitation was at 465 nm and emission at 529 nm. For NBD-PG (B) excitation was at 463 nm and emission at 530 nm. The data points represent the average of two (A) and three (B) experiments each. In (B) the error bars are standard deviations. For clarity the data points have been staggered slightly (0.2 C°).

centration was quite consistent from one experiment to the next, although the exact values of anisotropy varied somewhat, (as indicated by the error bars in Figs. 1–3, which correspond to standard deviation of the data). Anisotropy profiles very similar to those illustrated in Fig. 1 were obtained when vesicles were sonicated at 60 watts for 2 min to yield small unilamellar vesicles (data not shown).

To further characterize the effect of SP-C on NBD-PC (and NBD-PG) in 7:1 DPPC/DPPG multilamellar vesicles, fluorescence intensity measurements were obtained as a function of temperature and SP-C concentration (Fig. 2). At temperatures within the range of 20°C to 35°C, the fluorescence intensity of NBD-PC in the DPPC/DPPG liposomes is low relative to its fluorescence at the phase transition (41°C). The fluorescence of NBD-PC or NBD-PG increases to a maximum at the phase transition as melting of the lipid progresses. The relative fluorescence intensity of NBD-PC at temperatures above T_m decreases with increasing temperature. A temperature-induced increase in fluorescence at temperatures below the phase transition is also apparent in the presence of SP-C. As SP-C concentration is increased, the temperature at which maximal fluorescence is reached decreases from 41°C, in the absence of SP-C, to approx. 36°C in the presence of 2% SP-C. As with the anisotropy data, the fluorescence intensity profile of NBD-PG in 7:1 DPPC/DPPG liposomes in the absence and presence of SP-C was similar to that of NBD-PC (Fig. 2B), but with slightly more sensitive to lower concentrations of SP-C. For both NBD-PC and NBD-PG, addition of SP-C to the model membrane consistently shifted the wavelength maxima to shorter wavelengths by a maximum of 3 nm for 2% SP-C at 20°C.

When NBD-containing fluorescent probes are concentrated in micelles, bilayers, or a domain within a bilayer, their fluorescence is greatly decreased due to self-quenching [25,26]. To test whether the low fluorescence observed at 20°C in 7:1 DPPC/DPPG vesicles was due to self-quenching of the NBD probe, fluorescence intensity was measured over a range of probe concentrations from 0.02 to 2.5 mol% relative to bulk lipid. The concentration dependent quenching of NBD-PC fluorescence in 7:1 DPPC/DPPG vesicles in the presence and absence of 2% SP-C is represented by Fig. 3A. In 7:1 DPPC/DPPG, NBD-PC is remarkably sensitive to self-quenching, with 50% quenching of fluorescence observed at 0.23 mol%. Addition of 2% (w/w) SP-C (or 0.4 mol% SP-C) to the 7:1 DPPC/DPPG vesicles results in decreased self-quenching at a probe concentration of less than 2 mol%. Extrapolation of the curve of (F_v/F_T) vs. concentration to zero mol% results in a value of (F_v/F_T) of 1.8 in the absence of SP-C and 2.1 in the presence of 2% SP-C. For NBD-PG, the value of $(F_v/F_T)_0$ was 2.1 in the absence of SP-C or 2.0 in the presence of SP-C. The quantity $(F_v/F_T)_0$ is proportional to the intrinsic fluorescence of the probe in the absence of self-quenching. Since $(F_v/F_T)_0$ is not significantly altered by the presence of SP-C, the lower fluorescence intensity in the absence of SP-C can be attributed to self-quenching.

The dependence of NBD-PC anistropy on probe concentration is shown in Fig. 3B. At low probe concentrations, including those used in the experiments in Figs. 1 and 2 (0.2 mol%), a large increase in anisotropy is observed in the presence of 2% SP-C, as compared to lipid alone. At higher NBD-PC concentrations the anisotropy curves in the presence or absence of SP-C appear to converge. By using the lowest practical probe concentrations, we minimize both the effects of self-quenching and of perturbation of the bulk bilayer by probe molecules.

Because NBD-PC and NBD-PG, with the NBD group located at the end of a six carbon acyl chain,

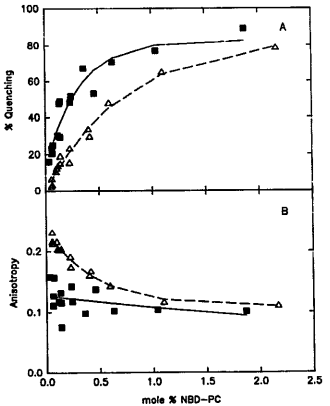

Fig. 3. Fluorescence quenching (A) and anisotropy (B) of NBD-PC in 7:1 DPPC/DPPG in multilamellar vesicles in the presence and absence of 2% SP-C as a function of NBD-PC concentration. % Quenching is calculated as described in methods. SP-C concentrations are (■) 0% and (△) 2% (w/w, protein/lipid). NBD-PC concentrations are expressed as mol% with respect to unlabelled lipid. Experiments were performed at 20°C. Data from the three separate experiments are shown.

have a relatively high critical micelle concentration of 32 nM [27], it was necessary to determine whether monomers of the NBD probe, not incorporated into vesicles, could be a contributing factor to the anisotropy changes. The fluorescence of solutions containing 8 to 110 nM NBD-PC, prepared by the ethanol injection method described above, was compared with the fluorescence of solutions of 7:1 DPPC/DPPG multilamellar vesicles containing the same total amount of NBD-PC. The fluorescence of the free probe was approx. 2% of the fluorescence of the vesicles throughout this range. The contributions of unbound NBD-PC to the parallel and perpendicularly polarized components of emitted light were measured and found to contribute no more than 2% error to the measured anisotropy, well within the range of experimental error (data not shown). In addition, the fluorescence of 330 nM NBD-PC prepared similarly was measured. This concentration of total NBD-PC corresponds to that used in the experiments shown in Figs. 1, 2 and 4. Multilamellar 7:1 DPPC/DPPG vesicles containing 0 or 1% SP-C were added to the NBD-PC dispersion and the fluorescence monitored for 5 h at 30°C. As the NBD-PC bound to the added vesicles, the fluorescence increased dramatically, in a manner similar to that observed by Arvinte et al. [25] for NBD-phosphatidylethanolamine. The fluorescence in the absence of vesicles was 3% or less that observed in the presence of vesicles, in agreement with published data on the NBD

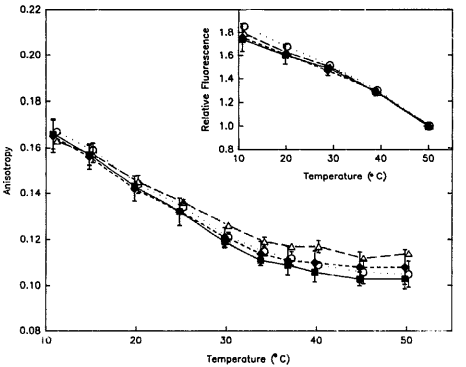

Fig. 4. Steady-state fluorescence anisotropy of NBD-PG in 6:1:1 DPPC/DPPG/eggPC multilamellar vesicles as a function of temperature and SP-C concentration and (inset) fluorescence intensity at 530 nm NBD-PG in 6:1:1 DPPC/DPPG/eggPC multilamellar vesicles as a function of temperature and SP-C concentration. SP-C concentrations are: 0% (■), 0.5% (○), 1.0% (◆), and 2.0% (△) (w/w, protein/lipid). Total lipid concentrations were 0.15 mg/ml. The data points in the graph represent the average of four experiments, or three separate experiments in the inset. In the inset, the ratio of fluorescence at each temperature to the fluorescence at 50°C (without Triton X-100) is plotted as mean ± S.E. For clarity the data points have been staggered slightly (0.2 °C)

probes [25,27]. The amount of free NBD-PC (or NBD-PG) present in the experiments in Figs. 1 and is less than that used in this titration experiment, and therefore, these values represent the maximum error introduced into the experiments by free NBD-PC or NBD-PG. No difference was seen in the rate of uptake of NBD-PC by vesicles containing 1% SP-C as compared with those lacking SP-C, although the fluorescence intensity of the SP-C-containing vesicles was higher (in agreement with Figs. 2 and 3).

Lipid mixtures, such as 6:1:1 DPPC/DPPG/eggPC, have been used to mimic the native lipid component of pulmonary surfactant since the amount of eggPC supplements the DPPC/DPPG mixture with an approximate amount of fatty acyl unsaturation found in surfactant phospholipids [6,28]. Therefore, it was of interest to examine the effect(s) of SP-C on such a lipid mixture using NBD-PC and NBD-PG as reporters of lipid organization. As illustrated in Fig. 4, the effect of the presence of eggPC on NBD-PG fluorescence anisotropy is readily apparent. As compared to the 7:1 DPPC/DPPG mixture, the phase transition is broadened, and the transition temperature is reduced to 22°C or below. The actual T_m cannot be determined from these data because the gel/fluid phase transition had begun at the lowest temperature studied, 10°C. At fluid phase temperatures (i.e. above 32°C), an increase in anisotropy with increasing SP-C concentration is apparent. Since a pure gel-phase was not reached during these experiments, and since the extent of phase separation of these samples is not known below fluid phase temperatures, determination of the effect of SP-C on the anisotropy of NBD-PG is not possible for temperatures below the transition temperature. However, the highest concentration of SP-C studied (2% (w/w)) caused more extensive broadening of the gel/fluid-phase transition. As shown in the inset of Fig. 4, the temperature dependence of NBD-PG fluorescence intensity in 6:1:1 DPPC/DPPG/eggPC vesicles differs from that of NBD-PG in 7:1 DPPC/DPPG liposomes in that the fluorescence decreased with increasing temperature over the temperature range studied. This indicates that NBD-PG was much less quenched in the DPPC/DPPG/eggPC preparations at lower temperatures, and therefore, little relief of quenching by SP-C was observed. The results obtained using NBD-PC as the reporter in the 6:1:1 DPPC/DPPG/eggPC mixture were similar to those of NBD-PG (data not shown).

Lifetime analysis

Fluorescence lifetime data of NBD-PC in 7:1 DPPC/DPPG and 6:1:1 DPPC/DPPG/eggPC vesicles (11°C), in the presence and absence of SP-C were consistent with a two lifetime model as determined by Gaussian fit analysis (Table I). Both the longer and shorter lifetime species (τ_1, and τ_2, respectively) were higher in value in the DPPC/DPPG/eggPC preparations than in DPPC/DPPG preparations. Addition of SP-C to either model lipid mixture resulted in an increase in both τ_1 and τ_2 of NBD-PC. These increases were most pronounced in the 7:1 DPPC/DPPG model membrane, where incorporation of 1% (w/w) SP-C increased both the τ_1 and τ_2 by nearly 40%. This is compared to an increase of only 9 to 10% for both the τ_1 and τ_2 of NBD in the 6:1:1 DPPC/DPPG/eggPC liposomes.

In order to characterize the effect of SP-C on NBD-PC lifetime components in varying lipid phases (i.e. gel-like and fluid phases), the temperature dependence of τ_1 and τ_2 in the absence and presence of SP-C was measured. Fig. 5 illustrates the effect of temperature and SP-C incorporation into 6:1:1 DPPC/DPPG/eggPC liposomes on τ_1 and mole fraction (α_1) of the long lifetime component. Over the entire temperature range studied, τ_1 was consistently higher in the presence of SP-C than the absence of protein. From 11°C to approximately 30°C, the values of τ_1 decreased dramatically in both preparations. The values of the long lifetime components remained fairly constant from 30°C to 40°C. The value of the short lifetime species was not significantly affected by either temperature or incorporation of SP-C into the DPPC/DPPG/eggPC liposomes (all values for τ_2 were between 1.3 to 1.0 ns from 20°C to 45°C; data not shown). In the presence and absence of SP-C the mole fraction of the long-life-

TABLE I

Gaussian best-fit parameters for two lifetime models of NBD-PC fluorescence decay in 7:1 DPPC/DPPG and 6:1:1 DPPC/DPPG/eggPC multilamellar vesicles in the absence and presence of bovine SP-C, T = 11°C

Symbols are as follows: $f_{1,2}$ = fraction of respective lifetime component; $\tau_{1,2}$ = lifetime centers (ns); $\alpha_{1,2}$ = mole fractions of the fluorophore decaying at the respective lifetime.

Sample	τ_1 (ns)	f_1	α_1	τ_2 (ns)	f_2	α_2	χ^2
7:1 DPPC/DPPG	6.44 (±0.06)	0.77	0.41	1.35 (±0.08)	0.23	0.59	4.92
6:1:1 DPPC/DPPG/eggPC	8.16 (±0.09)	0.88	0.66	2.22 (±0.10)	0.12	0.34	1.65
7:1 DPPC/DPPG + 1% SP-C	8.84 (±0.10)	0.85	0.56	1.96 (±0.11)	0.15	0.44	3.31
6:1:1 DPPC/DPPG/eggPC + 1% SP-C	8.88 (±0.12)	0.89	0.68	2.35 (±0.14)	0.11	0.32	2.74

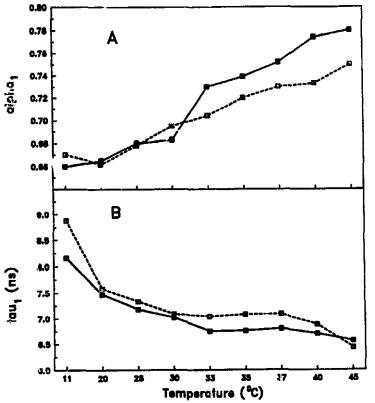

Fig. 5. Temperature dependence of τ_1 and α_1 of NBD-PC in 6:1:1:DPPC/DPPG/eggPC in the absence (■) and presence (□) of 1% bovine SP-C (w/w protein/total lipid). Excitation and emission wavelengths of NBD-PC were 325 nm and 490 nm, respectively.

time component increased with increasing temperature, with the addition of SP-C resulting in a more gradual, nearly linear, increase in α_1. Between 11°C and 30°C, no difference in the mole fraction of the long lifetime species was observed upon addition of SP-C; however, at 32°C and above, SP-C significantly reduced the proportion of the NBD-PC long lifetime species.

Rotational correlation times

Differential phase and modulation polarization measurements offer a means of monitoring the lateral pressure experienced by a probe molecule in its local environment. Differential phase and modulation data may be used to calculate the rate of depolarizing rotation of the fluorescent probe molecule as the rotational rate slows in more rigid environments. In especially restrictive sites the fluorophore may exhibit residual polarization even at times much longer than the fluorescence lifetimes. Such limiting anisotropy (r_∞) is commonly observed for probes in lipid bilayers. Higher lateral pressure imposes increasing order upon the phospholipid chains and upon probe molecules embedded within the bilayer as well. Hence, calculation of r_∞ from phase and modulation data provides a method for monitoring changes in lateral pressure. Accordingly, r_∞ was calculated for the NBD-PC probe using several rotational models. Parameters for anisotropy decay, as calculated using the hindered model (i.e. Eqn. 3), are summarized in Table II. For these calculations, each lifetime component was allowed one or two rotational correlation times. In all cases, the fit was not sufficiently improved by including two rotations for the long lifetime component (χ^2 did not decrease by more than 10%). Therefore, the results presented (in Table II) were calculated based on one rotational component for the long lifetime species. The limiting anisotropy values given in Table II correspond only to the long lifetime component since the short lifetime component did not exhibit an r_∞ regardless of the absence or presence of SP-C. Phase modulation data for both the DPPC/DPPG and DPPC/DPPG/eggPC model membrane preparations at 11°C show substantial r_∞ components to the long lifetime species. These r_∞ components are increased once SP-C is incorporated into the liposomes. These data suggest that SP-C exerted a static ordering effect within the headgroup region of the membrane bilayers.

The non-infinite rotational correlation times (θ_1 and θ_2) of NBD lifetime components (τ_1 and τ_2, respectively) are an indication of the dynamic order within the environment of the fluorophore. Values of θ_1 and θ_2 of NBD-PC in DPPC/DPPG/eggPC vesicles increased slightly upon inclusion of SP-C, but for the probe in 7:1 DPPC/DPPG liposomes, both θ_1 and θ_2 nearly doubled in value upon addition of SP-C. These results indicate that SP-C induced a modest decrease

TABLE II

Rotational correlation times and r_∞ values of NBD-PC in 7:1 DPPC/DPPG and 6:1:1 DPPC/DPPG/eggPC multilamellar vesicles in the absence and presence of 1% (w/w) SP-C, at 11°C

θ_1 and θ_2 represent the average rotational correlation times corresponding to the components with lifetimes τ_1 and τ_2, respectively (see Table I); the order parameter, S_2 is calculated from r_∞ and r_0 (= 0.380) using Eqn. 4.

Lipid mixture	SP-C	θ_1 (ns)	θ_2 (ns)	r_∞	χ^2	S_2
7:1 DPPC/DPPG	-	1.39 (±0.02)	0.095 (±0.004)	0.097	1.23	0.505
	+	2.60 (±0.03)	0.161 (±0.007)	0.142	1.08	0.612
6:1:1 DPPC/DPPG/eggPC	-	2.49 (±0.06)	0.054 (±0.002)	0.114	2.34	0.548
	+	3.31 (±0.08)	0.131 (±0.02)	0.132	2.79	0.589

in the rotational rate of the fluorophore. Therefore, incorporation of SP-C into the liposomes caused a slight increase in the dynamic order of the lipids.

Discussion

The data presented in this paper demonstrate the effects of surfactant-associated protein SP-C on the organization of lipids in two model membrane systems of similar composition to pulmonary surfactant, as determined by steady-state and time-resolved fluorescence measurements of the membrane probes NBD-PC and NBD-PG. Changes in fluorescence lifetimes, intensity, anisotropy and rotational correlation times of the NBD moiety reflect alterations in the dynamic structure of the lipid bilayer.

In order to determine SP-C-induced perturbations in lipid organization, it was necessary to characterize the fluorescence properties of the NBD fluorophore in the model membranes in the absence and presence of SP-C. Quenching experiments with aqueous quenchers [29] and spin-labelled lipids [22] have shown that in a major conformer of several NBD probes, including NBD-PC, the NBD ring is folded towards the bilayer surface. The fluorescence lifetimes of NBD-PE (phosphatidyl ethanolamine) in liposomes and in water/ethanol mixtures of various compositions have been studied by Arvinte et al. [25]. In solution, the wavelength maximum was shifted to shorter wavelength, and the fluorescence intensity and the single observed lifetime increased with decreasing solvent polarity. In liposomes, two lifetimes were observed. Both lifetimes decreased with increasing NBD-PE concentrations, and the mole fraction of probe contributing to the shorter lifetime increased due to self-quenching effects, as NBD-PE concentrations were increased over the range of 0–25 mol% NBD-PE [25]. In the experiments reported here, very much lower probe concentrations were used; however, the uniform acyl chain packing of DPPC/DPPG bilayers, and the location of the NBD group on the end of a 6-carbon acyl chain in the NBD-PC and NBD-PG probes, produce the self-quenching observed even at low probe concentrations. The two lifetimes observed for NBD-PC in liposomes (Table I) are similar to those observed for NBD-PE [25]. It is possible that the two lifetime species can be attributed to different conformers of the NBD probe, with the longer lifetime arising from the NBD moiety in a conformation that buries it in a less polar environment. Alternatively, the short lifetime species could arise exclusively from self-quenching. Both lifetimes increase on addition of SP-C to 7:1 DPPC/DPPG vesicles, an effect which could arise from (1) decreased self-quenching, or (2) from a probe conformation exposing the NBD moiety to a less polar environment.

Two distinct differences between gel and fluid phase lipids may account for either the preferential occurrence of the long-lifetime conformer or the decrease in self-quenching in the fluid phase. Since the phospholipid acyl chains are more disordered in the fluid than in the gel phase, they may better accommodate the irregular shape of the probe molecule when it is folded into the lipid bilayer interior. From this perspective, the gel phase lipids tend to exclude the probe molecules due to the uniformity of packing of acyl chains in the gel phase. Secondly, the lateral pressure is higher within the gel phase than in the fluid phase [30]. The increased pressure within the acyl region of gel phase lipids may cause the probe to adopt a more superficial conformation or form self-quenched domains. The relative hydrophilicity of the NBD fluorophore makes these probes sensitive to changes in lipid order in the more polar regions of the bilayer. Although any fluorescent probe will perturb the bilayer to some extent, the very low concentrations which we have used in all experiments other than the self-quenching experiments should minimize the perturbation, while being very sensitive to perturbations caused by added protein.

The addition of SP-C to the 7:1 DPPC/DPPG vesicles results in an increase the fraction of the NBD probes in the longer lifetime conformer, an increase the lifetimes of both conformers, and a small blue shift in wavelength maximum of NBD fluorescence. These effects can be explained by a disordering of the acyl chain region produced by SP-C, introducing packing defects which relieves self-quenching of the NBD probes and allow the NBD probes to adopt a more buried conformation. The shift in wavelength maximum is also consistent with a less polar environment of the NBD moiety [18]. Additionally, SP-C causes an increase in steady-state anisotropy of the NBD probes in the gel phase, which is also detectable in time-dependent experiments as an increase in the rotational correlation times and the r_∞ of the fluorophore. This partial immobilization of the lipids together with the apparent disordering of the acyl chain region may imply a differential effect of SP-C on the headgroup region and the interior of the bilayer. An alternative, but not exclusive, interpretation is that SP-C increases the lateral pressure specifically in the headgroup region of the bilayer, forcing the NBD fluorophore into a more buried conformation. This interpretation is discussed below.

Inclusion of SP-C into the 6:1:1 DPPC/DPPG/eggPC model membrane has little effect on the distribution of probe conformations at temperatures between 11 and 33°C but lowers the proportion of the long lifetime conformer by 15 mol% above 33°C. The fact that no effect on distribution was seen in the DPPC/DPPG/eggPC vesicles may be a result of the inability to achieve pure gel phase lipids at the temper-

atures studied. Additionally, the presence of a mixture of acyl chain lengths and degrees of unsaturation in eggPC would tend to disorder the acyl chain region of the bilayer, minimizing the additional effect of SP-C. The effects of SP-C on the rotational correlation times and r_∞ remain evident even in the presence of eggPC, indicating that the ordering of the headgroup region of the bilayer by SP-C is independent of its effects on the lifetime of the probe.

In the absence of SP-C, there is a sharp change in the value of α_1, the fraction of the long-lifetime conformer, between 30 and 33°C in 6:1:1 DPPC/DPPG/eggPC, probably reflecting the melting of a separate domain of the membrane lipids. The presence of SP-C smooths out this transition, implying that SP-C may actually reduce the formation of domains, or perhaps, modulate their melting properties by maintaining more rigidity in the polar region of the bilayer. In contrast to the other hydrophobic surfactant protein SP-B [31], SP-C did not demonstrate a strong preferential interaction with NBD-PG.

The r_∞ value is related to the order parameter S_2 for the NBD fluorophore according to the equation:

$$r_\infty / r_0 = (S_2)^2 \tag{4}$$

This equation is strictly applicable for fluorophores in which the transition dipole for either absorption or emission is parallel to the symmetry axis of the probe [32], a condition not met by the NBD probe, however, the presumptive orientation of the long wavelength intramolecular charge-transfer transition is along the amino-nitro group axis, which is approximately coaxial with the direction of attachment of the NBD moiety to the acyl chain, about which depolarizing rotations occur. Moreover, the actual value of S_2 will differ from the calculated value by constant term. The values of S_2 calculated by Eqn. 4, (Table II), indicate that SP-C induces a substantial increase in static ordering in the gel phase 7:1 DPPC/DPPG model membrane, and a smaller increase in the 6:1:1 DPPC/DPPG/eggPC membranes at 11°C. The order parameter S_2 has been correlated with the lateral pressure within the membrane [30]. Lateral pressure, which results from steric repulsion between neighboring acyl chains, requires that the polar head groups of the phospholipids become more closely packed [33]. An increase in lateral pressure induced by SP-C invites analogy to its ability to increase surface pressure (thereby decreasing surface tension) in monolayers, although the nature of the relationship between surface pressure in a monolayer and lateral pressure in a bilayer is not well defined. The increase in S_2 upon addition of SP-C may be interpreted as due to relative immobilization of the lipid headgroup region with a subsequent increase in lateral pressure.

In 7:1 DPPC:DPPG vesicles NBD-PC (Fig. 3A) and NBD-PG (data not shown) are remarkably sensitive to self-quenching, with 50% quenching of fluorescence observed at 0.23 mol%. In contrast, a more than 30-fold greater concentration (8 mol%) of C_{12}-NBD-PC (1-acyl-2-(12-[*N*-(7-nitrobenz-2-oxa-1,3-diazol-4-yl)amino]dodecanoyl)phosphatidylcholine) was required to obtain 50% quenching in dioleoylphosphatidylcholine [26]. The uniformity of acyl chain packing in the dipalmitoyl phospholipids used in our experiments is presumably sufficient to exclude NBD-PC and NBD-PG, causing them to form microdomains of self-quenched molecules, in equilibrium with unquenched molecules present within the bulk lipid. Addition of pulmonary surfactant protein SP-C to the 7:1 DPPC/DPPG vesicles results in an increase in fluorescence intensity which arises from a decrease in self-quenching (Fig. 3A). The SP-C molecules presumably disrupt the lipid structure in their vicinity, forming a domain of lipid which is less closely packed, and which does not exclude NBD-probe molecules. For self-quenching to be decreased by this mechanism, the disturbed lipid domain must be sufficiently large to allow dilution of NBD-PC or NBD-PG molecules, so that they are no longer self-quenched.

At low NBD-PC concentrations, a large increase in anisotropy is observed on addition of SP-C (Figs. 1 and 3) to 7:1 DPPC/DPPG vesicles. This reflects a decrease in mobility in the headgroup region of the lipid bilayer in the vicinity of SP-C, in agreement with the time dependent results discussed above. The decrease in anisotropy in the 2% SP-C samples at high probe concentration is probably related to the presence of self-quenched domains enriched for probe molecules. In addition, the concentration of probe may be sufficient to cause major perturbation to lipid packing in the bilayer. The melting temperature of lipid in 7:1 DPPC/DPPG vesicles is shifted to lower temperature in the vicinity of SP-C, as shown by both the anisotropy vs. temperature (Fig. 1) and fluorescence intensity vs. temperature curves (Fig. 2). The broadening of the phase transition by SP-C results in a disordering of the bilayer relative to pure lipid at 37°C. The effects of SP-C on lipid mobility and phase transition are not surprising for a highly hydrophobic peptide [34–36] but the magnitude of the interaction is unusual. The effect of SP-C is readily observable at a lipid/protein molar ratio of 500:1. By comparison, mellitin causes no discernable change in the anisotropy of DPH in lipid bilayers below about 40:1 molar ratio [34,35].

Recent work of Curstedt et al. [12] demonstrates that human SP-C is palmitoylated on the two cysteine residues near the amino terminus of the peptide. These groups are conserved in porcine, bovine and human SP-C peptide sequences. Thus, the interactions of SP-C with phospholipids may be mediated by interaction of

the hydrophobic, valine rich domain but may also be influenced by interactions between phospholipid and fatty acyl chains of SP-C. These acyl chains would only reach half way through a bilayer, whereas SP-C itself is likely to span the bilayer.

In these studies reported we have found SP-C to have two effects on lipid structure in vesicles; first, it partially disorders the acyl chain region of the bilayer; and second, it increases rigidity in the head group region of the bilayer. If these effects can be extrapolated to monolayer conditions, the first effect would promote spreading on expansion of the lung, and the second would help stabilize the lipid film against collapse at end expiration. Both of these are activities at which SP-C excels in monolayer experiments.

Acknowledgements

Programs of Excellence in Molecular Biology, HL41496, Research Training in Perinatology MD07200 (J.E.B.), and ALA/ATS Research Grant RG0038 (J.E.B.), Molecular and Cellular Biology Training Grant HL07527 (A.D.H.).

References

1 Goerke, J. (1974) Biochim. Biophys. Acta 334, 241–261.
2 Harwood, J.L. and Richards, R.J. (1985) Biochem. Soc. Trans. 13, 1079–1081.
3 Notter, R.H. (1984) in Pulmonary Surfactant (Robertson, B., Van Golde, L.M.G. and Batenburg, J.J., eds.), pp. 17–65, Elsevier Science Publishers, Amsterdam.
4 Harwood, J.L. (1987) Prog. Lipid Res. 26, 211–256.
5 Notter, R. and Finkelstein, J.N. (1984) J. Appl. Physiol.: Respir. Env. Exerc. Physiol. 57, 1613–1624.
6 Tanaka, Y., Takei, T., Aiba, T., Masuda, K., Kiuchi, A. and Fujiwara, T. (1986) J. Lipid Res. 27, 475–485.
7 Whitsett, J.A., Ohning, B.L., Ross, G., Meuth, J., Weaver, T., Holm, B.A., Shapiro, D.L. and Notter, R.H. (1986) Pediatr. Res. 20, 460–467.
8 Hawgood, S., Benson, B.J., Schilling, J., Damm, D., Clements, J.A. and White, R.T. (1987) Proc. Natl. Acad. Sci. USA 84, 66–70.
9 Yu, S.-H. and Possmayer, F. (1986) Biochem. J. 236, 85–89.
10 Glasser, S.W., Korfhagen, T.R., Weaver, T.E., Clark, J.C., Pilot-Matias, T., Meuth, J., Fox, J.L. and Whitsett, J.A. (1988) J. Biol. Chem. 263, 9–12.
11 Johansson, J., Jornvall, H., Eklund, A., Chistensen, N., Robertson, B. and Curstedt, T. (1988) FEBS Lett. 232, 61–64.
12 Curstedt, T., Johansson, J., Persson, P., Eklund, A., Robertson, B., Lowenadler, B. and Jornvall, H. (1990) Proc. Natl. Acad. Sci. USA 87, 2985–2989.
13 Glasser, S.W., Korfhagen, T.R., Weaver, T.E., Pilot-Matias, T., Fox, J.L. and Whitsett, J.A. (1987) Proc. Natl. Acad. Sci. USA 84, 4007–4011.
14 Curstedt, T., Johansson, J., Barros-Soderling, J., Robertson, B., Nilsson, G., Westberg, M. and Jornvall, H. (1988) Eur. J. Biochem. 172, 521–525.
15 Notter, R.H., Shapiro, D.L., Ohning, B. and Whitsett, J.A. (1987) Chem. Phys. Lipids 44, 1–17.
16 Pagano, R.E. and Sleight, R.G. (1985a) Science 229, 1051–1057.
17 Pagano, R.E. and Sleight, R.G. (1985b) Trends Biochem. Sci. 10, 421–425.
18 Chattopadhyay, A. (1990) Chem. Phys. Lipids 53, 1–15.
19 Ross, G.F., Notter, R.M., Meuth, J. and Whitsett, J.A. (1986) J. Biol. Chem. 261, 14283–14291.
20 Klausner, R.D. and Wolf, D.E. (1980) Biochemistry 19, 6199–6203.
21 Parasassi, T., Conti, F. and Gratton, E. (1986) Cell. Mol. Biol. 32, 103–108.
22 Chattopadhyay, A. and London, E. (1988) Biochim. Biophys. Acta 938, 24–34.
23 Gratton, E. and Limkeman, M. (1983) Biophys. J. 44, 315–324.
24 Lakowicz, J.R., Cherek, H. and Maliwal, B. (1985) Biochemistry 24, 376–383.
25 Arvinte, T., Cudd, A. and Hildenbrand, K. (1986) Biochim. Biophys. Acta 860, 215–228.
26 Nichols, J.W. and Pagano, R.E. (1981) Biochemistry 20, 2783–2789.
27 Nichols, J.W. (1985) Biochemistry 24, 6390–6398.
28 Notter, R.H., Finkelstein, J.N. and Taubold, R.D. (1983) Chem. Phys. Lipids 33, 67–80.
29 Chattopadhyay, A. and London, E. (1987) Biochemistry 26, 39–45.
30 Fulford, A.J.C. and Peel, W.E. (1980) Biochim. Biophys. Acta 598, 237–246.
31 Baatz, J.E., Elledge, B. and Whitsett, J.A. (1990) Biochemistry 29, 6714–6720.
32 Heyn, M.P. (1979) FEBS Lett. 108(2) 359–364.
33 Marcelja, S. (1974) Biochim. Biophys. Acta 367, 165–176.
34 Jahnig, F. (1981) Biophys. J. 36, 347–357.
35 Jahnig, F., Vogel, H. and Best, L. (1982) Biochemistry 21, 6790–6798.
36 Lentz, B., Clubb, K.W., Alford, D.R., Hochli, M. and Merssner, G. (1985) Biochemistry 24, 433–442.